MULTI-TASK RANK LEARNING FOR IMAGE QUALITY ASSESSMENT

Long Xu[1], Jia Li[2, 3], Weisi Lin[4], Yongbing Zhang[5], Lin Ma[6], Yuming Fang[7], Yun Zhang[8], Yihua Yan[1]*

[1]Key Laboratory of Solar Activity, National Astronomical Observatories, Chinese Academy of Sciences, Beijing, China
[2]State Key Laboratory of Virtual Reality Technology and Systems, School of Computer Science and Engineering, Beihang University, Beijing, China
[3]International Research Institute for Multidisciplinary Science at Beihang University, Beijing, China
[4]Department of Computer Engineering, Nanyang Technological University, Singapore
[5]Graduate School at Shenzhen, Tsinghua University, Shenzhen, China
[6]Huawei Noah's Ark Lab, Hong Kong
[7]School of Information Technology, Jiangxi University of Finance and Economics, Nanchang, China
[8]Shenzhen Institutes of Advanced Technology, Chinese Academy of Sciences, Shenzhen, China
{lxu, yyh}@nao.cas.cn; jiali@buaa.edu.cn; WSlin@ntu.edu.sg; zhang.yongbing@sz.tsinghua.edu.cn; forest.linma@gmail.com; fa0001ng@e.ntu.edu.sg; yun.zhang@siat.ac.cn

ABSTRACT

In practice, multiple types of distortions are associated with an image quality degradation process. The existing machine learning (ML) based image quality assessment (IQA) approaches generally established a unified model for all distortion types, or each model is trained independently for each distortion type by using single-task learning, which lead to the poor generalization ability of the models as applied to practical image processing. There are often the underlying cross relatedness amongst these single-task learnings in IQA, which is ignored by the previous approaches. To solve this problem, we propose a multi-task learning framework to train IQA models simultaneously across individual tasks each of which concerns one distortion type. These relatedness can be therefore exploited to improve the generalization ability of IQA models from single-task learning. In addition, pairwise image quality rank instead of image quality rating is optimized in learning task. By mapping image quality rank to image quality rating, a novel no-reference (NR) IQA approach can be derived. The experimental results confirm that the proposed Multi-task Rank Learning based IQA (MRLIQ) approach is prominent among all state-of-the-art NR-IQA approaches.

Index Terms— Rank learning, image quality assessment, machine learning, MOS, pairwise comparison

1. INTRODUCTION

Three categories of NR IQA approaches were presented in the literature. The ***first*** category of approaches takes the behavior of specific distortions into consideration. In [1], Sheikh *et al*. employed wavelet statistical model to capture the distortion introduced by JPEG 2000. Liang *et al*. [2] combined the sharpness, blurring, and ringing measurements together to evaluate the visual quality of the JPEG 2000 coded image. Brandao *et al*. [3] proposed an NR-IQA approach based on the DCT domain statistics to evaluate the quality of JPEG coded image. In [4], R. Ferzli *et al*. integrated the concept of just noticeable blur into probability summation model to measure sharpness/ blurriness. The ***second*** category of approaches uses quality aware clustering. They group the image patches of training set into the given number of classes based on local image features, such as histogram of oriented gradients (HoG), difference of Gaussian (DoG) and Gabor filter. Each cluster center has a quality score which is derived from the qualities of image patches falling into this cluster. Associating cluster centers with their qualities, the researchers established a codebook. Patches of a test image look up codebook to search the most similar codewords and retrieve the associated quality values. In [5], a visual codebook associated Gabor filter based local appearance descriptors with MOS. The authors of [6] used FSIM [7] instead of MOS as image patch quality to establish codebook. The ***third*** category is to utilize machine learning (ML) tool to map image features onto image qualities. In [9], Moorthy *et al*. proposed to use support vector machine (SVM) and support vector regression (SVR) to learn a classifier and an ensemble of regressors for image distortion classification and computing quality of specific distorted image. It deploys summary statistics derived from an on natural scene statistics (NSS) wavelet coefficient model, using a two-step framework for IQA: distortion classification and distortion specific IQA regression. In [8], Tang *et al*. proposed an approach similar to [9] but with more elaborate features,

including distortion texture statistics, blur/noise statistics and histogram of each subbands of image decomposition. In our previous effort [1], a novel IQA model applying rank learning and pairwise comparison (PC) to IQA was investigated.

In existing works on ML based IQA, two issues have been intensively studied. One is the image feature. The so-called NSS image feature [9] was widely used and its variants [8] were proposed. The other concerns learning algorithm. The popular one learning algorithm is applying SVM/SVR to identify distortion type and pool image feature into a number result, where a SVR is preceded by a SVM classifier to classify distortion type and perform distortion-aware IQA [9]. In [8], the authors raised a more sophisticated image feature while processing all kind of distortion types with the same model without distortion type discrimination. This two kinds of algorithms are associated with at least one of the problems as following: 1) arranging training set into several clusters, there would be less training samples for each training task, which possibly results in overfitting and weak generalization capability of trained model; 2) the common features shared by different distortion types are not exploited efficiently. Therefore, a combination of "emphasize individuality" and "exploit commonness" would create better performance.

Toward this end, we propose a multi-task rank learning approach for IQA (MRLIQ). In this approach, we construct multiple IQA models, each of which is responsible for one distortion type in order that each model can accurately describe the specific characteristics of each distortion type. Different from single-task learning approach, these IQA models are integrated into a multi-task learning task, and they are trained simultaneously. Thus, the relatedness and information sharing across multiple training tasks are effectively exploited to improve the generalization of each model. In addition, departing from the conventional machine learning based IQAs, the proposed approach targets at pairwise (PC) image quality rank instead of numerical image quality rating to establish the optimization target, which follows our previous work [1].

The rest of this paper is arranged as follows. Section II describes the proposed MRLIQ in detail. Section III presents the experimental results. And, the final section concludes this paper.

2. MULTI-TASK RANK LEARNING FOR IMAGE QUALITY ASSESSMENT

Single-task learning is independently trained on the subset of the whole training set, which ignores the intrinsic relatedness among different tasks. For example, one can train several IQA models, each of which is responsible for one distortion type. There are two problems in such a processing. One is that there would be ***less training samples allocated to each task***, which possibly results in overfitting and harms the generalization capability of learned model. The other is that the ***common features among different distorted images are not exploited***. Multi-task learning is different from signal task learning in that the multiple tasks are trained simultaneously instead of independently. The fact is that all samples (with all distortion types) are used for training each task (each sample concerning a weighting to each task), while only samples with the same distortion type are used in single task scheme. Therefore, the multi-task scheme can exploit underlying intrinsic relatedness among multiple tasks and capture shared/common information of training data. It has attracted extensive attention in many domains, such information retrieval (IR) and visual saliency modeling [10]. To the best of our knowledge, it has not been applied to IQA yet.

2.1. Single-task rank learning

In [1], a single task ranking learning algorithm was proposed, where only one task and therefore one ranking model were trained. Given a subjective image database, we represent the image features $\{x_i \in R^L\}$ and the corresponding MOSs $\{y_i \in R\}$, i=1, 2, …, M. Thus, the goal of a rank learning based IQA can be described as identifying the ranks of $\{x_i\}$ with respect to $\{y_i\}$. Toward this end, we infer a ranking function $\varphi : x \rightarrow$ R trained on the basis of $\{x_i, y_i\}$, to assign rank order to each x_i. That is, $\varphi(x_i) > \varphi(x_j)$ indicates that x_i ranks higher than x_j with respect to image quality. In [1], only one task and therefore one ranking model φ was trained on all distorted images as

$$\min_{\omega} \left\{ \sum_{u \neq i}^{M} [\boldsymbol{y}_u < \boldsymbol{y}_i]_1 [\varphi(\boldsymbol{x}_u) \geq \varphi(\boldsymbol{x}_i)]_1 \right\}, \quad (1)$$

for all types of distortions (e.g., 5 distortions for LIVE image database), where φ is usually assumed to be a linear function, i.e., $\varphi(x) = \omega^T \cdot x$ for simplicity, and both x and ω are vectors length of L. This distortion-unaware model is inferior to the distortion-specific model in that the significant characteristics difference are among different distortions.

2.2. Multi-task rank learning

For distortion-specific purpose, we can directly apply the proposed single task learning [1] to learn a specific model for each distortion. Such a model is distortion-specific, and therefore has better prediction accuracy. We assume to group the training set into K clusters $\{S_j\}$, j=1,2,…,K with respect to their distortion types, and a specific model is trained on each cluster to have an specific ranking function φ_j. Let the i-th image in the j-th cluster x_i^j (i=1,2,…,m_j, j=1,2,…,K) $\sum_{j=1}^{K} m_j = M$), and the corresponding label (MOS or DMOS in IQA) y_i^j, the j-th model φ_j is trained on the cluster S_j consisting of m_j distorted images and associated labels $\{(x_i^j, y_i^j)\}$ as:

$$\min_{\omega_j} \left\{ \sum_{u \neq i}^{m_j} \left[\boldsymbol{y}_u^j < \boldsymbol{y}_i^j \right]_1 \left[\varphi_j(\boldsymbol{x}_u^j) \geq \varphi_j(\boldsymbol{x}_i^j) \right]_1 \right\}, \quad (2)$$

where $\varphi_j(x) = \omega_j{}^T \cdot x$. Comparing to (1), m_j training samples only concerning the j-th task are used for training φ_j in (2). Applying (2) to K clusters, there would be K models each of which is specific for each distortion type. Although the model is distortion-specific, there would be two problems as mentioned earlier in the beginning of this section.

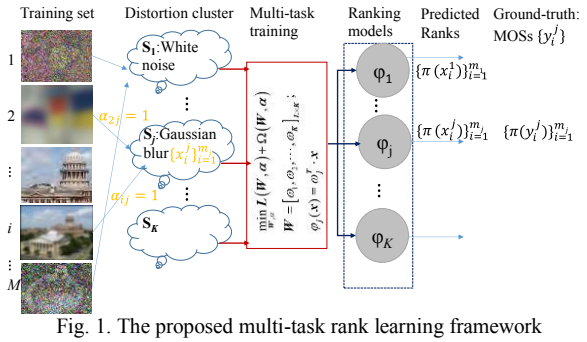

Fig. 1. The proposed multi-task rank learning framework

Therefore, we refer to a multi-task learning scheme to jointly train multiple models to avoid these two problems in this work.

Comparing to single task, multi-task learning means that: ***1)*** all models $\{\varphi_j, j = 1,2,\dots,K\}$ concerned are trained jointly instead of independently (see (1) and (2)); ***2)*** all training sampling are used for training each model. Obviously, a sample distorted by a certain distortion type should contribute more than others distorted by other distortion types to the model specialized by this distortion type. To explore the contribution of a given sample with a certain distortion type to each of the models, we define a matrix of distortion-cluster labels $\boldsymbol{\alpha}=\{\alpha_{ij}\}$. Initially, we set $\alpha_{ij} \in \{0, 1\}$, where $\alpha_{ij} = 1$ indicates a sample x belongs to the cluster S_j. After applying a weight α_{ij} to a sample, this sample could be used in all training tasks.

Fig. 1 describes the framework of multi-task learning. $\{\pi(x_i^j)\}_{i=1}^{m_j}$ represents the rank list of $\{x_i^j\}_{i=1}^{m_j}$ of the j-th cluster by using corresponding φ_j. $\{\pi(y_i^j)\}_{i=1}^{m_j}$ is the rank list of MOSs by comparing their numerical values, which is the ground-truth in the proposed learning algorithm. From Fig. 1, the images are grouped into K clusters. The models $\{\varphi_j\}$ are trained together instead of independently as (2). Note the red box in Fig. 1, all samples are involved in training task, and the multi-task training outputs K models. Each model can rank the image in the corresponding cluster. After ranking each cluster, the rank list of the whole training set can be obtained.

For the convenience of statement, we firstly formulate the whole optimization function, and then detail each element. Let $\boldsymbol{W}$ be a $L\times K$ matrix with the j-th column equals to ω_j, the bold $\boldsymbol{\alpha}$ be a $M\times K$ matrix with the i-th row equals to $\{\alpha_{ij}\}_{j=1}^{K}$which is a K-dimensional vector. Each of the entries of this vector represents the weight of the i-th sample as to the j-th task. Therefore, the objective for jointly training multiple IQA models can be formulated as

$$\begin{aligned} &\min_{\boldsymbol{W},\alpha} \boldsymbol{L}(\boldsymbol{W},\boldsymbol{\alpha})+\Omega(\boldsymbol{W},\boldsymbol{\alpha}) \\ &\boldsymbol{s.t.}\quad \sum_{j=1}^{K}\alpha_{ij}=1;\forall \boldsymbol{i}\in[1,\boldsymbol{M}] \\ &\alpha_{ij}\in\{0,1\};\forall \boldsymbol{j}\in[1,\boldsymbol{K}] \end{aligned} \quad , \tag{3}$$

where $L(\boldsymbol{W},\boldsymbol{\alpha})$ is the empirical loss and $\Omega(\boldsymbol{W},\boldsymbol{\alpha})$ is the penalty term.

2.2.1 Empirical loss

The empirical loss accounts for the falsely ranked image pairs with regard to their MOSs as

$$\boldsymbol{L}(\boldsymbol{W},\boldsymbol{\alpha})=\sum_{i=1}^{M}\sum_{j=1}^{K}\alpha_{ij}\sum_{u=1,u\neq i}^{M}\left[\boldsymbol{y}_u<\boldsymbol{y}_i\right]_{\mathrm{I}}\left[\boldsymbol{\omega}_j^T\boldsymbol{x}_u\geq\boldsymbol{\omega}_j^T\boldsymbol{x}_i\right]_{\mathrm{I}}, \tag{4}$$

where $[p]_{\mathrm{I}}=1$ if p holds; otherwise $[p]_{\mathrm{I}}=0$. In (4), each pair of images (x_u and x_i, $\boldsymbol{u}\neq\boldsymbol{i}$) in the whole training set (M samples) are compared. Their MOSs are given by y_u and y_i respectively. The ranks of y_u and y_i gives the ground-truth of the comparison of x_u and x_i. If the ranks of $\boldsymbol{\omega}_j^T\boldsymbol{x}_u$ and $\boldsymbol{\omega}_j^T\boldsymbol{x}_v$ conflicts with the ground-truth, the empirical loss $L(\boldsymbol{W},\alpha)$ increases.

2.2.2 Distortion clustering

To group images with the same distortion type into the same cluster, the penalty term is defined as

$$\Omega_1=\frac{1}{\boldsymbol{M}}\sum_{u,v=1;u\neq v}^{M}\sum_{j=1}^{K}\left(\alpha_{uj}-\alpha_{vj}\right)^2\cos\left(\boldsymbol{x}_u,\boldsymbol{x}_v\right), \tag{5}$$

where $\cos(x_u, x_v)$ denotes the similarity of the u-th and the v-th image (u, v=1,2,…,M), which is computed as the cosine distance between two feature vectors x_u and x_v. If these two images have the same distortion types (e.g., $\alpha_{uj}=\alpha_{vj}=1$) are correctly classified into the corresponding cluster, there is no penalty ($\alpha_{uj}-\alpha_{vj}=0$). Otherwise, i.e., two objects belonging to the same distortion category was mistakenly classified into two different clusters, the penalty would increase.

2.2.3 Model correlation

To solve the problem of lack the generalization ability with training these clusters respectively, taking an appropriate sharing of information across training tasks can avoid overfitting and improve the performance of each model. Then the penalty term can be defined as

$$\begin{aligned}\Omega_2=\frac{1}{\boldsymbol{K}}\sum_{i\neq j}^{K}\sum_{u\neq v}^{M}&\left[\boldsymbol{y}_u<\boldsymbol{y}_v\right]_{\mathrm{I}}\times \\ &\left[\boldsymbol{\omega}_i^T\boldsymbol{x}_u\geq\boldsymbol{\omega}_i^T\boldsymbol{x}_v\right]_{\mathrm{I}}\left[\boldsymbol{\omega}_j^T\boldsymbol{x}_u\geq\boldsymbol{\omega}_j^T\boldsymbol{x}_v\right]_{\mathrm{I}}\end{aligned} . \tag{6}$$

The influence of this penalty is two-fold. First, a sample mistakenly predicted by most models will be emphasized in training φ_i (i.e., a large $\sum_{j\neq i}\left[\boldsymbol{y}_u<\boldsymbol{y}_v\right]_{\mathrm{I}}\times\left[\boldsymbol{\omega}_j^T\boldsymbol{x}_u\geq\boldsymbol{\omega}_j^T\boldsymbol{x}_v\right]_{\mathrm{I}}$). This ensures the diversity of training samples for φ_i, leading to improved generalization ability. Second, a sample successfully predicted by most models will be ignored in training φ_i (i.e., a small $\sum_{j\neq i}\left[\boldsymbol{y}_u<\boldsymbol{y}_v\right]_{\mathrm{I}}\times\left[\boldsymbol{\omega}_j^T\boldsymbol{x}_u\geq\boldsymbol{\omega}_j^T\boldsymbol{x}_v\right]_{\mathrm{I}}$). This guarantees the diversity of different models. With this penalty term, each task is actually related to all the training samples with different weights as stated in [10], leading to improved performance.

With these penalty terms, the overall penalty can be written as the weighted linear combination of them.

2.3. Training process

By plugging (4) to (6) back (3), we encounter a non-convex optimization problem due to the function $[p]_{\mathrm{I}}$. As in [10], the

Boolean terms related to variable ω is replaced by their upper bounds to facilitate the optimization as:

$$[\omega_j^T x_u \le \omega_j^T x_v]_I \le \mathrm{e}^{(\omega_j^T x_u - \omega_j^T x_v)} \triangleq \eta_{uv}^j \quad (7)$$

where the exponential upper bound is used since it is convex and can facilitate the optimization. After the terms containing the variable ω in (3) being replaced, the empirical loss function would turn out to be convex. In addition, two variable $\boldsymbol{W}$ and $\boldsymbol{\alpha}$ are correlated in (3). Thus, the expectation maximization (EM) algorithm is employed to optimize $\boldsymbol{W}$ and α alternately.

Firstly, the distortion-cluster labels $\boldsymbol{\alpha}$ are initialized since the distortion types are known for all images. Then, $\boldsymbol{W}$ is initialized by minimizing (4) without penalty consideration. After initialization, $\boldsymbol{W}$ and $\boldsymbol{\alpha}$ are optimized iteratively using EM algorithm. The detail algorithm steps can refer to our previous work on saliency estimation [10].

It should be pointed that the models derived from (3) are only for ranking images with respect to their qualities instead of assigning a physical quantity (like PSNR) to each image. Thus, these models are used to rank images of the training set firstly. Then, a set of new models are deduced to describe the relation between ranks and MOSs of images by using interpolation techniques, such as polynomial curve fitting. For simplicity, the same notation is used to represent both quality ranking and quality assessment hereinafter.

Given a new image, we have to choose a proper model for predicting its quality. As claimed in [9], the NSS feature and SVM classifier can efficiently identify the distortion type of an image. Thus, we adopt the classifier (a SVM classifier) in [9] to choose a proper model to estimate the quality of the input image. The classifier on LIVE image database and codec of extracting NSS feature is accessible by [15].

3. EXPERIMENTAL RESULTS AND DISCUSSIONS

To evaluate the proposed algorithm, we perform our experiments on LIVE image database [11] which consists of 29 reference images, each image has 5 distortion types (JPEG, JP2K, white noise (WN), Gaussian blur (GB) and fast fading (FF) channel distortions) and 5/6 distortion levels per type.

The images in database are divided into training sets and testing sets. A training set consists of 80% of the reference images and their associated distorted versions, and a testing set consists of the remaining 20% of the reference images and their associated distorted versions. In order to ensure that MRLIQ is robust across content and is not biased by the specific train-test split, random 80% train-20% test split is repeated 100 times on LIVE image database. The media PLCC, SROCC and RMSE values across these 100 times training processes are tabulated in Tables 1-2, for each distortion category, as well as across distortion categories. In Tables 1-2, MRLIQ represents the proposed algorithm with only NSS feature in training model. We also compared MRLIQ with the state-of-the-art approaches, including four FR-IQA metrics: PSNR, SSIM, MS-SSIM and VIF, six NR-IQA metrics: DIIVINE [9], LBIQ [8], CBIQ [5], BLIINDS-II [16], TMIQ [18] and NIQE [19].

As can be seen from Tables 1-2, although MRLIQ is not the best on all distortion types, it ranks within top-2 and without a large margin from the best one. Remarkably, MRLIQ is better than DIIVINE on all distortion types except "WN" distortion. It should be pointed that these two approaches have the same features, which implies that the proposed multi-task rank learning approach contributes to the achievement. The very meaningful point is that we take a fundamental departure from the traditional learning scheme by introducing pairwise rank learning and multi-task learning into IQA. The MRLIQ would be expected with more improvement space considering more elaborate feature and algorithmic optimization.

Table 1. Median PLCC across 100 train-test combinations on the LIVE IQA database

	JP2K	JPEG	WN	Blur	FF	All
PSNR	0.8762	0.9029	0.9173	0.7801	0.8795	0.8592
SSIM	0.9405	0.9462	0.9824	0.9004	0.9514	0.9066
MS-SSIM	0.9746	0.9793	0.9883	0.9645	0.9488	0.9511
VIF	0.9790	0.9880	0.9920	0.9760	0.9720	0.9610
CBIQ	0.8898	0.9454	0.9533	0.9338	0.8951	0.8955
LBIQ	0.9103	0.9345	0.9761	0.9104	0.8382	0.9087
BLIINDS-II	**0.9386**	0.9426	0.9635	0.8994	0.8790	0.9164
DIIVINE	0.9233	0.9347	**0.9867**	0.9370	0.8916	0.9270
TMIQ	0.8730	0.8941	0.8816	0.8530	0.8234	0.7856
NIQE	0.9370	**0.9564**	0.9773	**0.9525**	0.9128	0.9147
MRLIQ	0.9368	0.9363	0.9402	0.9389	**0.9495**	**0.9300**

Table 2. Median SROCC across 100 train-test combinations on the LIVE IQA database

	JP2K	JPEG	WN	Blur	FF	All
PSNR	0.8646	0.8831	0.9410	0.7515	0.8736	0.8636
SSIM	0.9389	0.9466	0.9635	0.9046	0.9393	0.9129
MS-SSIM	0.9627	0.9785	0.9773	0.9542	0.9386	0.9535
VIF	0.9670	0.9820	0.9840	0.9730	0.9630	0.9640
CBIQ	0.8935	**0.9418**	0.9582	0.9324	0.8727	0.8954
LBIQ	0.9040	0.9291	0.9702	0.8983	0.8222	0.9063
BLIINDS-II	**0.9323**	0.9331	0.9463	0.8912	0.8519	0.9124
DIIVINE	0.9123	0.9208	**0.9818**	0.9337	0.8694	0.9250
TMIQ	0.8412	0.8734	0.8445	0.8712	0.7656	0.8010
NIQE	0.9172	0.9382	0.9662	0.9341	0.8594	0.9135
MRLIQ	0.9213	**0.9281**	0.9242	**0.9357**	**0.9125**	**0.9276**

4. CONCLUSIONS

In this paper, we have investigated multi-task rank learning for IQA. Due to the significant difference between the statistics of different distorted images, the multi-task learning training individual computer model for each type of distortion is more accurate than the methods without distortion type discrimination. In addition, multiple models are trained simultaneously on all training samples with the consideration of sharing common feature and highlighting specific feature of each task, which will enhance the generality capability of trained models. Moreover, MRLIQ takes a fundamental and interesting departure from the traditional learning framework on numerical rating optimization.

5. REFERENCES

[1] L. Xu, W. Lin, J. Li, X. Wang, Y. Yan, Y. Fang, "Rank learning on training set selection and image quality assessment", *ICME*, 2014.

[2] H. R. Sheikh, A. C. Bovik, and L. Cormack, "No-reference quality assessment using nature scene statistics: JPEG 2000", *IEEE Trans. Image Process.*, vol. 14, no. 11, pp. 1918-1927, Nov. 2005.

[3] L. Liang, S. Wang, J. Chen, S. Ma, D. Zhao, and W. Gao, "No-reference perceptual image quality metric using gradient profiles for JPEG 2000", *Signal Processing: Image Communication*, vol. 25, no. 7, pp. 502-516, Aug. 2010.

[4] T. Brandao, and M. P. Queluz, "No-reference image quality assessment based on DCT domain statistics", *Signal Processing*, vol. 88, no. 4, pp. 822-833, Apr. 2008.

[5] P. Ye, and D. Doermann, "No-reference image quality assessment using visual codebooks," *IEEE Trans. Image Process.*, vol. 21, no. 7, pp. 3129-3138, 2012.

[6] W. Xue, L. Zhang, and X. Mou, "Learning without Human Scores for Blind Image Quality Assessment," *CVPR*, 2013.

[7] Lin. Zhang, L. Zhang, X. Mou and D. Zhang, "FSIM: a feature similarity index for image quality assessment," *IEEE Trans. Image Process.*, vol. 20, no. 8, pp. 2378-2386, Aug., 2011.

[8] H. Tang, N. Joshi, and A. Kapoor, "Learning a Blind Measure of Perceptual Image Quality," *CVPR*, 2011.

[9] A.K. Moorthy, and A. C. Bovik, "Blind image quality assessment: From natural scene statistics to perceptual quality," *IEEE Trans. Image Process.*, vol. 20, no. 12, pp. 3350-3364, 2011.

[10] J. Li, Y. H. Tian, T. Huang, and W. Gao, "Cost-Sensitive Rank Learning from Positive and Unlabeled Data for Visual Saliency Estimation," *IEEE Signal Process. Lett.*, vol. 17, no. 6, pp. 591-594, 2010.

[11] LIVE Image Quality Database. Available [Online]: http://live.ece.utexas.edu/research/quality/subjective.htm.

[12] A. Ninassi, P. Le Callet, and F. Autrusseau, Subjective Quality Assessment-IVC Database 2005. Available [Online]: http://www2.irccyn.ecnantes.fr/ivcdb.

[13] Y. Horita, K. Shibata, Y. Kawayoke, and Z. M. P. Sazzad, MICT Image Quality Evaluation Database 2000. Available [Online]: http://mict.eng.u-toyama.ac.jp/mict/index2.html.

[14] D. M. Chandler and S. S. Hemami, A57 Database 2007. Available [Online]: http://foulard.ece.cornell.edu/dmc27/vsnr/vsnr.html.

[15] http://live.ece.utexas.edu/resources/index.htm.

[16] M. Saad, A. C. Bovik, and C. Charrier, "Blind image quality assessment: A natural scene statistics approach in the DCT domain," *IEEE Trans. Image Process.*, vol. 21, no. 8, pp. 3339–3352, 2012.

[17] A. Mittal, A. K. Moorthy, and A. C. Bovik, "No-reference image quality assessment in the spatial domain," *IEEE Trans. Image Process.*, vol. 21, no. 12, pp. 4695-4708, Dec. 2012.

[18] A. Mittal, G. S. Muralidhar, J. Ghosh, and A. C. Bovik, "Blind image quality assessment without human training using latent quality factors," *IEEE Signal Process. Lett.*, vol. 19, 2011, pp. 75–78.

[19] A. Mittal, R. Soundararajan, and A. C. Bovik, "Making a "completely blind" image quality analyzer," *IEEE Signal Process. Lett.*, vol. 20, no. 3, pp. 209-212, 2013.